# It is hard to be small: Inbreeding depression depends on the body size in a threatened songbird

Justyna Kubacka[1]*, Larissa S. Arantes[2,3], Magdalena Herdegen-Radwan[4], Tomasz S. Osiejuk[4], Sarah Sparmann[2,5] and Camila J. Mazzoni[2,3]

[1] Museum and Institute of Zoology of the Polish Academy of Sciences, Twarda 51/55, 00-818 Warszawa, Poland

[2] Berlin Center for Genomics in Biodiversity Research, Königin-Luise-Straße 6-8, 14195 Berlin, Germany

[3] Leibniz Institute for Zoo and Wildlife Research, Alfred-Kowalke-Straße 17, 10315 Berlin, Germany

[4] Department of Behavioural Ecology, Faculty of Biology, Adam Mickiewicz University, Uniwersytetu Poznańskiego 6, 61-614 Poznań, Poland

[5] Leibniz Institute of Freshwater Ecology and Inland Fisheries, Müggelseedamm 310, 12587 Berlin Berlin, Germany

* corresponding author, e-mail: jkubacka@miiz.waw.pl

## Abstract

While inbreeding is known to affect individual fitness and thus population extinction risk, studies have under-represented non-model species of conservation concern, and rarely sought conditionality of inbreeding depression. Here, using SNPs identified with RAD-seq, we determined inbreeding depression in a threatened bird, the aquatic warbler *Acrocephalus paludicola*, and whether its magnitude depends on phenotypic and environmental factors. We found that the inbreeding coefficient (*F*) of adults with small tarsi was negatively associated with the seasonal breeding success (in males) and clutch size (in females), with the respective decrease in fitness in the most inbred relative to the least inbred individuals of ~89% and ~12%. In contrast, in adult males, for the average tarsus, wing and mass, support was low for *F* to be related to the long-term return rate to breeding grounds. For mean phenotypic covariates and male density, we also found low evidence that *F* is associated with the annual breeding success. Likewise, there was little support that mother *F* is related to egg hatch success and nestling survival, and – for average phenotypic traits, rainfall, temperature and nest density, and accounting for breeding peak – to clutch and fledged brood sizes. For nestlings, animal models showed that *F* is more negatively related to tarsus under higher

temperatures and its effect varies by study year. However, for average brood size, temperature, rainfall and prey abundance, and when controlling for nestling sex, breeding peak and mother *F*, evidence for nestling *F* and tarsus association was weak. We conclude that (1) inbreeding depression on fitness components is stronger in smaller-bodied individuals, (2) considering interaction with phenotypic and environmental variables enables more accurate estimation of inbreeding depression, and (3) the inbreeding depression estimates will inform extinction risk analysis and conservation actions for the aquatic warbler.

## Introduction

Inbreeding results from mating between kin, non-random mating or division of a population into isolated groups (Keller & Waller 2002). It leads to increased genomic homozygosity and accumulation of harmful mutations, which are typically recessive and thus more often expressed in highly homozygous, inbred individuals. Consequently, more inbred individuals have compromised fitness. Inbreeding depression is found across plant and animal taxa (Ralls *et al.* 1988, Keller & Waller 2002) and is especially strong in wild populations (Crnokrak & Roff 1999). Inbreeding negatively affects key fitness components, such as sperm quality (Gage *et al.* 2006, Hinkson & Poo 2020), embryo development (Noordwijk & Scharloo 1981, Kruuk *et al.* 2002, Hemmings *et al.* 2012a), juvenile survival (Kruuk *et al.* 2002, Kennedy *et al.* 2014), annual reproductive success (Huisman *et al.* 2016, Niskanen *et al.* 2020), and lifetime reproductive success (Grueber *et al.* 2010, Huisman *et al.* 2016, Harrisson *et al.* 2019). Therefore, inbreeding depression decreases population viability and contributes to extinction risk (Westemeier *et al.* 1998, Brook *et al.* 2002, O'Grady *et al.* 2006, Nonaka *et al.* 2019), and evaluating its impact is of particular importance in populations of conservation concern.

Inbreeding depression is expected to be more pronounced in harsher environments or individuals of lower condition (Armbruster & Reed 2005). For example, low food availability and high number of competitors enhance the inbreeding depression on survival in Darwin's finches (*Geospiza sp.*) (Keller *et al.* 2002). A long-term study on the great tit (*Parus major*) found that inbreeding by environment interactions, while generally weak, are stronger in adverse conditions more closely related to fitness (Szulkin & Sheldon 2007). Laboratory experiments on insects showed that inbreeding effects on offspring survival increase with mother age (Fox & Reed 2010) and environmental toxicity (Nowak *et al.* 2007). However, evaluation of the conditionality of inbreeding depression in wild populations has not been frequent, while determining its magnitude across individual traits and environmental conditions would yield more accurate inbreeding depression estimates, especially in threatened populations.

Here, we determine the strength of inbreeding depression on fitness-related traits in an IUCN-threatened songbird, the aquatic warbler *Acrocephalus paludicola*, a habitat specialist breeding in fen mires and a long-distance migrant (Le Nevé *et al.* 2018, Tanneberger *et al.* 2018b). Following the gradual disappearance of fens, which accelerated especially over the past 100-200 years due to peat extraction, changes in hydrological regime, drainage, eutrophication and succession, the extent of occurrence of the species shrank considerably (Tanneberger *et al.* 2018a). This led to a steep decline in the population size, amounting to 95% only between 1950-80, and its extinction from the western Europe by the end of the 20th century (Briedis & Keišs 2016, Flade *et al.*

2018). Today, the breeding range of the aquatic warbler is constrained to the east-central Europe, which holds c. 98% of the global population estimated at 12200 singing males (Flade *et al.* 2018). A recent study (Kubacka *et al.* 2024) demonstrated that genetic diversity in the species is low and comparable to that of other threatened bird species (Evans & Sheldon 2008, Vitorino *et al.* 2019). As it is habitat specialists that are more strongly affected by loss of genetic diversity (Matthews *et al.* 2014, Pflüger *et al.* 2019), it is crucial to determine the magnitude of inbreeding depression in the aquatic warbler. In addition, alongside the depleted genetic diversity, the high asymmetry of the male reproductive success (Dyrcz *et al.* 2002, 2005, Kubacka *et al.* 2025) and the promiscuous mating system (Leisler & Schulze-Hagen 2011) are expected to increase variation in the inbreeding rates, which facilitates detection of inbreeding depression (Balloux *et al.* 2004), thus making the species a good study model. Finally, the aquatic warbler faces a broad range of environmental conditions, as the breeding season strides the cool spring and the hot summer, water levels on the fen are changeable, and nests are built on the ground and thus exposed to environmental factors, all of which enable studying the conditionality of inbreeding depression.

Specifically, we aimed at 1) assessing the relationship of adult inbreeding rates with the reproductive success and survival, and of nestling inbreeding rates with the body size; 2) evaluating whether inbreeding depression is conditioned by phenotypic variables corresponding to individual quality and by environmental variables that are expected to affect adult survival and fecundity, and offspring body size; and 3) quantifying the inbreeding load and change in fitness associated with inbreeding.

## Methods

### *Study area and sampling*

The study was conducted between May-August of 2017-2023, in the Biebrza Valley (Poland), which holds about 25% of the global breeding population of the aquatic warbler. The breeding habitat is permanently water-logged open fen mire and to a less extent wet meadows, all dominated by sedges *Carex* spp. Three study areas were used, referred to as Ławki (N 53º17′11.4″, E 22º33′49.2″), Szorce (N 53º17′34.8″, E 22º37′15.9″) and Mścichy (53º25′41.7″ E 22º30′17.0″). Each study area consisted of two 10-20-hectare (ha) study plots, totalling 70 ha.

Between May-July of 2017-2019, adult individuals (past their 1st calendar year) were caught with mist-nets and marked with unique metal and colour rings. They were blood-sampled through puncture of the brachial vein with a sterile needle and collecting approx. 10-120 ul of blood with a capillary. Each blood sample was immediately placed in a vial with an o-ring seal, containing 2 ml of

96% EtOH, and shaken to avoid formation of large clots. We measured tarsus length (from the notch on the metatarsus to the top of the bone above the folded toes, with a calliper to the nearest 0.1 mm), wing length (with a ruler to the nearest mm) and body mass (with an electronic Kern CM 150-1N balance to the nearest 0.1 g).

Nests were located by search and observation of alarming females, every 2-7 days in each plot from late May to early June, and from late June until the end of July. We distinguished two breeding peaks, which correspond to the first and second breeding attempts that are typically separated by about 10 days when no nests are initiated (Kubacka *et al.* 2014). Nests were monitored every 1-5 days. In nests found at the egg stage or on day 1 post-hatch (day 0 being the last day when most offspring in the nest were still eggs), we determined the clutch size, hatched brood size and nestling survival (number of chicks surviving from hatching to fledging). After day 1 the risk is higher that a nestling dies and is removed by the female, which biases estimation of the above traits. In all the nests, we recorded the fledged brood size as the number of nestlings seen on the last check when the brood was still in the nest, as long as on the following check the nest did not bear any traces of predation and was recorded empty not earlier than on day 12 post-hatch (i.e. 3 days before the expected fledging).

In 2017-2018, the tarsus and body mass of chicks were measured, as above, on days 2, 5 and 9 post-hatch, which fall at the beginning, in one third and in two thirds of the nest stage, respectively. Only nestlings from nests found at the egg stage or day 1-2 post-hatch were included in the analysis. We used the nestling tarsus length as it is one of the proxies for structural body size in birds (Rising & Somers 1989, Senar & Pascual 1997) and predicts survival to reproductive maturity (Gebhardt-Henrich & Richner 1998). Chicks were blood-sampled (approx. 10-80 µl) on day 9 post-hatch, as above.

Between May-July of 2018-2023, we searched the study plots and their surroundings up to 150 m off plot border for colour-ringed adults with the search effort of 0.2-3.9 person-hours per ha. The colour-ring code was read with an 80-mm-lens and 20-60 magnification scope. The position of each resighted individual was stored in a GPS receiver. We measured the long-term return rate by the number of years during which a given adult individual was resighted or recaught in the study plots, or in other breeding areas – as determined from the Polish Bird Ringing Database, over 4 years following the first observation as adult.

We obtained the daily sum of rainfall in mm and average daily temperature from the Polish Institute of Meteorology and Water Management (IMGW). To assess food abundance, in 2017-2018 we sampled arthropod prey within c. 30 m from the nest by sweep-netting (1 sweep per 1 second)

on 3 radially oriented transects between 3 m of the nest and 50 steps away from the nest. Collected arthropods were placed in a plastic bag, frozen upon arrival from the field, determined to the order and counted. We then quantified the amount of preferred prey as the total number of insects from the taxonomic groups known to be selectively brought by females to nestlings: *Odonata*, *Aranea*, *Lepidoptera* and *Orthoptera* (Schulze-Hagen *et al.* 1989). We estimated the male density with QGIS 3.10.7 (QGIS Development Team 2020) as the average number of ringed males observed within 100 m of each ringed male's position, and the nest density as the number of nests found per 10 ha of study plot. Following our previous study (Kubacka *et al.* 2025), based on all the captures and resights of the males, we determined the number of encounters of a male per plot in each breeding season, to account for excess zeros in the male breeding success (see *Statistical analysis*). We suspected that the low father-to-offspring assignment rate (see *Results*) could be caused mainly by late arrivals of some males to the study areas. Individuals with a low number of encounters were first captured during the second breeding attempt, or were rarely seen in the study plots.

### *DNA extraction and molecular sex identification*

DNA was isolated with the Xpure™ Blood Mini kit (A&A Biotechnology, Poland). 200-300 µl of blood suspended in 96% EtOH were used per individual and the proteinase K digestion time was 2-3 hours. The remaining steps were performed according to the manufacturer's protocol. We analysed DNA of 175 adult males (1 was ringed as a chick), 320 chicks (2 were resighted as adult males) from 79 nests and 105 adult females. DNA concentration was measured with a Picogreen (Invitrogen) or Qubit (Thermo Fisher Scientific) instrument.

Sex of nestlings was determined by PCR amplification of sex-specific sequences in the CHD-W (c. 370 bp, females only) and CHD-Z genes (c. 330 bp, both sexes) (Griffiths et al. 1998) with a PCR kit (Eurx, Poland). Electrophoresis of PCR products ran for 90 mins at 100 V in a 3% agarose gel stained with Simply Safe (Eurx, Poland) and the gel was photographed under UV light.

### *Molecular marker identification and genotyping*

To determine inbreeding rates and assign paternity, we used single nucleotide polymorphisms (SNPs), determined with 3-enzyme restriction site-associated sequencing (3RAD) (Bayona-Vásquez *et al.* 2019, Glenn *et al.* 2019). Inbreeding estimated with genomic markers better predicts the identity by descent and decrease in fitness, compared to inbreeding rates inferred from the pedigree (Hemmings *et al.* 2012b, Kardos *et al.* 2015, Huisman *et al.* 2016). First, we constructed a reference

173 genomic library, i.e. a catalogue of reliable loci excluding potential paralogs and artefactual alleles,
174 according to the Reduced-Representation Single-Copy Orthologs (R2SCOs) method (Driller *et al.*
175 2021), with modifications. We sequenced 2x300 bp reads for three females to reconstruct the entire
176 locus by merging overlapping reads, using samples with high DNA concentration (75.9, 53.7 and 76.6
177 ng/µl), each representing a different study location. After normalising the samples to 20 ng/µl, we
178 split each into 5 digestion reactions (200 ng each), totalling 1 µg digested DNA. The enzymes XbaI,
179 EcoRI-HF and NheI were used for the digestion, which ran at 37°C for 2 hours. Each digestion
180 reaction was ligated with a unique XbaI and EcoRI adapter pair (i.e. double-indexed) and the 5
181 reactions were pooled and purified (0.8x PCRclean magnetic beads - GCbiotech). We performed a
182 PCR with P5 and P7 customised ligation check primers, to ensure that the digestion was successful.
183 Each pooled sample was size-selected (350-580 bp) on a BluePippin machine (Sage Science). Each
184 size selection product was then split into 4 reactions and in a single-cycle PCR we added an iTru5-8N
185 index (with 8 random nucleotides, to mark unique DNA template molecules and remove PCR
186 duplicates during the bioinformatic analysis) (Hoffberg *et al.* 2016). After purification (0.8x beads) an
187 additional PCR step (8 cycles) completed the Illumina adapters with a unique iTru7 P7 primer per
188 reaction and a P5 primer (which has a flow cell binding site sequence) common to all the reactions.
189 The 4 PCR replicates of each sample were then pooled, purified (0.8x beads) and quantified (Qubit –
190 Thermo Fisher Scientific). Finally, the pools were sequenced with the Illumina MiSeq V3 at 600
191 cycles, yielding a total of 3.6 M reads per sample.

192 Next, we constructed population libraries (Supplementary Online Resource 1), consisting of
193 the remaining 597 samples. DNA concentration was normalised to 20 ng/ul or less (at least 8.14
194 ng/µl). We followed the protocol described above (Bayona-Vásquez *et al.* 2019), with modifications,
195 and produced 9 population libraries, which were processed in 3 batches. The libraries were
196 sequenced with 2x150 bp on Illumina instruments; 15% of PhiX was used to increase sequence
197 diversity. The number of sequenced reads obtained from each library is presented in Table S1a.

198

199 ***Bioinformatic analysis***

200 We first constructed a reference locus catalogue using the R2SCOs method (Driller *et al.* 2021),
201 which allowed us to select a set of high-quality single-copy orthologous loci to be used as reference
202 for the population analysis. The R2SCOs pipeline included de-replication of the pre-processed and
203 size-selected sequences (range 250-370 bp, for which we obtained comparable and high coverage),
204 setting the minimum coverage per unique sequence to define a putative allele equal to 3; and
205 clustering and definition of putative loci using the intra-specific identity threshold of 90%. As a next

206 step, the pipeline applies a set of filters to remove loci that are prone to generate spurious results
207 due to issues of either biological or technical background. Aiming to avoid sex-biased genotypes that
208 might interfere with the population analyses (Faux *et al.* 2020), we removed all the R2SCOs loci that
209 mapped to the sex chromosomes of the Eurasian blackcap (*Sylvia atricapilla*) genome (GenBank
210 accession number GCA_009819655.1). The final reference contained 10997 loci.

211 The raw data from the population libraries was mapped against the PhiX genome to filter
212 any remaining read from the Illumina library control. Next, we performed adapter trimming using
213 the Cutadapt software (Martin 2011). Then, reads were attributed to individuals based on the in-line
214 barcodes using FLEXBAR (Dodt *et al.* 2012). In part of the libraries (Supplementary Online Resource
215 1), PCR duplicates were filtered out using the Python script Filter_PCR_duplicates.py
216 (https://github.com/BeGenDiv/Arantes_et_al_2020). The 4 replicates were then concatenated. The
217 forward and reverse reads were merged with overlapping regions of at least 30 bp and maximum
218 length of 249 using the software PEAR (Zhang *et al.* 2014). All the merged reads (<249 bp) were
219 considered short fragments that were out of the target range, and we continued analysing the
220 unassembled read pairs, which were filtered for minimum quality (Q>30) and trimmed to 142 bp
221 with a minimum length of 130 bp using Trimmomatic (Bolger *et al.* 2014). We checked the presence
222 of the XbaI and EcoRI restriction sites in the paired-read ends using the script
223 checkRestrictionSites.py (https://github.com/BeGenDiv/Arantes_et_al_2020) and filtering out any
224 fragment resulting from star activity or NheI digestion. Finally, reads containing the internal
225 restriction site of XbaI, EcoRI or NheI were removed using the Filter_Reads.py script
226 (https://github.com/BeGenDiv/Arantes_et_al_2020). The filtered reads were mapped against the
227 reference locus catalog constructed with the R2SCOs method, using Bowtie2 (Langmead *et al.* 2009)
228 with default parameters and the flags '-no-mixed' and '-no-discordant'. In order to select a common
229 range of high-coverage loci for all individuals belonging to different libraries, we checked the length
230 distribution of the loci based on the .sam files, and extracted the range 250-310 bp with *samtools*
231 (Danecek *et al.* 2021) and a bash *awk* command.

232 We analysed the mapped reads with Stacks (Catchen *et al.* 2011, 2013), using the reference-
233 based pipeline. Genotypes were called and filtered with ref_*map.pl*, which uses the *gstacks* and
234 *populations* modules. In *gstacks*, the *var_alpha* (alpha threshold for discovering SNPs) was set to
235 0.01, and all the samples were assumed to belong to one population, because of the extensive gene
236 flow known in the aquatic warbler (Kubacka *et al.* 2024). Otherwise, default parameters were used.
237 In *populations*, we used: the minimum percentage of individuals in a population required to process
238 a locus r= 0.8, to avoid high missingness; the minimum number of populations a locus must be
239 present in to be processed p= 1; and the minimum minor allele frequency required to process a

nucleotide site at a locus min-maf= 0.005, which ensured that an allele is present in at least three samples to be processed (Rochette & Catchen 2017). To obtain independent SNPs, we wrote only the first SNP in a locus. The remaining parameters were retained at their defaults. After calling genotypes, we generated mean depth per individual with Vcftools (Danecek *et al.* 2011), to inspect coverage distribution. We removed 1 individual with mean depth <10 and repeated the SNP-calling step. We obtained 6267 loci, of which 4179 variant sites (SNPs) were retained after the *populations* filter, with mean ±SE observed heterozygosity in variable positions of 0.141 ±0.002. We checked whether individuals with the lowest coverage (mean depth of ≥10x and <30x, N= 46) affect loci-calling, by running *ref_map.pl* without them. The number of SNPs called without these individuals was 4171 and the mean ±SE observed heterozygosity was 0.143 ±0.002; we therefore retained them for further analysis.

We then used Vcftools for further SNP filtering (Table S1b). We removed genotypes with mean depth per SNP <10x and loci with >20% missing data. Next, we filtered out sites (N= 6) of mean depth >115, which formed the tail of the depth distribution, to remove potential collapsed paralogs. In the R environment (R Core Team 2024), with the *dartR* package (Gruber *et al.* 2018) we checked whether the loci are in the Hardy-Weinberg equilibrium (HWE), applying the false discovery rate correction and p-value of 0.05. Most loci not in HWE were heterozygote-deficient and we found a positive correlation between the locus Fis and missingness (r= 0.38), which decreased to r= 0.13 after the HWE-violating loci were removed. As this is indicative of null alleles, which artefactually lower heterozygosity (Waples 2015, De Meeûs 2018), we proceeded without the HWE-violating SNPs. Finally, using VCFtools, we calculated loci-pairwise $r^2$ to inspect distribution of linkage disequilibrium. The mean ±SD of $r^2$ was 0.003±0.012. We excluded one randomly selected SNP from each pair for which $r^2$ was >0.3, to remove the tail of $r^2$ distribution (Fig. S1). The final dataset consisted of 2948 SNPs (Table S1b). The mean ±SD read depth per locus and individual are provided in Fig. S2.

## Paternity assignment

We selected a set of informative SNPs to maximise the statistical power of parentage assignment (Andrews *et al.* 2018, Thrasher *et al.* 2018). With Vcftools (Danecek *et al.* 2011), we filtered out SNPs with minor allele frequency <0.3, as rare SNP variants are not informative in parentage assignment (Huisman 2017), and missingness >0.1. The number of SNPs after filtering was 333 (Table S1b). Typically, 100-200 SNPs suffice for parentage assignment (Huisman 2017, Flanagan & Jones 2019). For 1 individual, which was RAD-sequenced twice, we removed the genotype with fewer loci typed.

273 The resulting genotypes dataset consisted of 320 offspring (316 with known mother) and 173
274 candidate fathers, with 1 mother typed in 88 SNPs and all the other individuals typed in >99 SNPs.
275 Paternity was then assigned with Cervus (Kalinowski *et al.* 2007), running the allele frequency
276 analysis, parentage analysis simulation and paternity analysis given known mother. The allele
277 frequency analysis showed the mean proportion of SNPs typed of 0.954. In the simulation, we
278 assumed: the allele frequencies generated in the previous step; 100000 offspring; 440 as the
279 average number of candidate fathers per offspring (based on the number of males assessed within
280 the study plots and 150 m around them, and summed over all the three study locations); 0.4 as the
281 proportion of candidate fathers sampled; 0.954 and 0.01 as the proportion of loci typed and
282 mistyped, respectively; 0.01 as the error rate in likelihood calculations; 88 as the minimum number
283 of typed loci; Delta as the statistic to determine confidence; and 99% and 95% as the strict and
284 relaxed confidence level, respectively. In the paternity analysis, we used the allele frequency and
285 simulation results generated in the previous steps. The offspring file contained candidate fathers,
286 and males known to not be sexually mature in the year when a given chick was born were excluded.
287 We ran the simulation and paternity analyses also for 95% and 80% strict and relaxed confidence
288 levels, respectively. In addition, we established paternity with Colony v. 2.0.7.1 (Jones & Wang
289 2010), providing information on known maternal sibships and excluded paternity, assuming
290 polygamy of both sexes, no inbreeding and default parameters otherwise. We quantified the male
291 seasonal breeding success as the number of offspring produced in the given year, as detected by
292 paternity assignment to the blood-sampled chicks.

293

294 ***Inbreeding rate and inbreeding load***

295 To assess inbreeding, we quantified the inbreeding coefficient *F* with a method of moments (Wang
296 2014) using the *–het* option in VCFtools (Danecek *et al.* 2011). To explore how well *F* corresponded
297 to inbreeding, with the R package *inbreedR* (Stoffel *et al.* 2016), we calculated $g_2$, an estimate of
298 identity disequilibrium which quantifies the covariance of heterozygosity at the studied loci
299 standardised by their average heterozygosity; hence, it corresponds to inbreeding variance in the
300 population (David *et al.* 2007). A correlation between a trait and heterozygosity will not arise when
301 $g_2 = 0$ (Szulkin *et al.* 2010). To avoid pseudoreplication, we used a dataset filtered to include all the
302 adult individuals and 1 nestling per nest. We used 1000 permutations over SNPs to evaluate whether
303 $g_2 > 0$ and 1000 bootstraps over individuals to determine its 95% confidence interval (CI).

304 To quantify the strength of inbreeding depression, we used the inbreeding load measured
305 with lethal equivalents (*B*) and percent change in fitness due to inbreeding ($\delta$) (Morton & Crow

306 1956, Keller & Waller 2002). Assuming that mutations at different loci have independent effects on
307 fitness, the logarithm of a fitness-related trait is predicted to show a linear negative relationship with
308 the inbreeding coefficient. The inbreeding load is quantified as the negative of the slope describing
309 this relationship. To compare inbreeding load between populations and studies, the concept of
310 lethal equivalents was coined. The effect of a mutation on fitness can be lethal or have partial
311 detrimental effects. One lethal equivalent is the average number of alleles in a population which
312 cause death of the homozygous individual. The inbreeding load equals the average number of lethal
313 equivalents per haploid gamete found in the studied population. We calculated *B* using Equation II in
314 Box 3 from Keller & Waller (2002), predictions weighted-averaged across all the models and
315 categorical levels (see *Statistical analysis*), and fitness values for the maximum and minimum
316 inbreeding rates in our dataset. For the survival traits, we used Poisson models with the logarithm
317 link function, which yield unbiased estimates of inbreeding load for binomial traits (Nietlisbach *et al.*
318 2019). The $\delta$ refers to the change in a fitness-related trait in inbred individuals compared to outbred
319 individuals (Keller & Waller 2002). We calculated $\delta$ for the most inbred compared to the least inbred
320 individuals in the dataset (Harrisson *et al.* 2019, Sin *et al.* 2021).

321

322 ***Statistical analysis***

323 We ran the analysis in the R environment 4.4.2 (R Core Team 2024) and applied the information-
324 theoretic approach, in which an a priori set of biologically plausible candidate models is built and
325 each model in the set obtains a relative rank indicating how well it explains the data (Burnham &
326 Anderson 2002). To rank models within a candidate set, we used the Akaike information criterion
327 corrected for small sample size (AICc) and – in animal models (see below) – the deviance information
328 criterion (DIC). In addition, we generated the following quantitative measures of relative support for
329 each model: model likelihood (relative likelihood of the model in the candidate set, given the data),
330 Akaike/DIC weight (ωAICc/ωDIC; probability that the given model is the best approximating model in
331 the candidate set), evidence ratio (showing the probability of the best model relative to other
332 models in the set) and cumulative AICc/DIC (sum of AICc/DIC weights of a given model and all the
333 higher-ranking models) (Symonds & Moussalli 2011).

334 Each candidate set included a null model assuming that the response variable is constant, or
335 that it varies with a variable strongly affecting the response that was common to all the models. All
336 the models in the set except the null model included *F*. For selected candidate sets, we restricted the
337 number of variables in a model to allow 10-15 data points per each non-intercept estimate and
338 reduce the risk of over-parametrisation; for models using the binomial distribution, we ensured that

339 there are 10-15 data points of the less probable event per estimate (Harrell 2015). To account for
340 model uncertainty, the estimates of regression coefficients and their confidence intervals were
341 weighted-averaged (by the ωAICc/ωDIC) across all the models in a set that contained the given term
342 (i.e. natural model-averaging), as we expected small effects (Grueber *et al.* 2011, Symonds &
343 Moussalli 2011). Model selection and averaging were carried out with package *AICmodavg*
344 (Mazerolle 2023). All the input numerical explanatory variables were standardised to the mean of
345 zero and SD of 1 (i.e. z-score standardisation). The weather variables, nest density and prey
346 abundance were z-score standardised within the year and breeding peak; in the chick tarsus analysis,
347 the weather variables were also standardised within the day. Sum contrasts were used (i.e. with the
348 intercept being the corrected mean), to enable comparison of effects of categorical and numerical
349 variables. For visualising interactions, predictions were calculated using packages *AICmodavg*
350 (Mazerolle 2023) and *MuMIn* (Bartoń 2019) for the model containing the term, on the link scale and
351 back-transformed. We visualised results with package *ggplot2* (Wickham 2016) and custom code.

352 We evaluated the relationship between *F* as an explanatory variable and the fitness-related
353 (male long-term return rate, male breeding success, clutch size, hatch success, nestling survival and
354 fledged brood size) and condition-related traits (chick tarsus on days 2, 5 and 9 post-hatch) as
355 response. We also determined whether the *F* effect is conditioned by phenotypic (tarsus, wing and
356 body mass in adults; sex in offspring) or environmental variables (male density, nest density, rainfall,
357 temperature, breeding peak, prey abundance and brood size). Candidate sets were built as follows:

358 (1) *Male inbreeding and long-term return rate*. We did not consider the female return rate due to
359 only 8 recoveries, which did not ensure a reliable regression analysis (Harrell 2015). The male 4-
360 year-return rate showed a right-skewed distribution. In order to select an appropriate count
361 model, following the recommendations by Zuur & Ieno (2021), we ran an intercept-only GLM
362 Poisson (*P*) model with log-link with the return rate as response, and calculated its
363 overdispersion and zero-inflation using package *DHARMa* (Hartig 2022). The *P* model showed
364 overdispersion (dispersion statistic 1.44, $P<0.001$) but no zero-inflation (ratio of observed to
365 simulated zeros 1.09, $P= 0.194$). We then ran an intercept-only negative-binomial (NB) model
366 using package *MASS* (Venables & Ripley 2002), which showed no overdispersion (1.00, $P=0.997$)
367 and no zero-inflation (1.00, $P= 1.000$). Therefore, we continued with the NB distribution to
368 construct a candidate model set. We included the following terms: body mass, tarsus and wing
369 length, ringing area and year, their interaction with *F*, *F* squared, body mass squared, tarsus
370 squared, and wing squared (Table S2a).
371 (2) *Male inbreeding and seasonal breeding success*. The male breeding success had a large number
372 of zeros and, corresponding to previous observations (Dyrcz *et al.* 2002, 2005, Kubacka *et al.*

373 2025), was right-skewed. We proceeded as in point (1) and constructed a null GLM *P* log-link
374 model with the number of encounters and ringing year as explanatory variables. The *P* model
375 was overdispersed (dispersion statistic 4.31, $P<0.001$) and zero-inflated (ratio of observed to
376 simulated zeros 1.70, $P<0.001$). We then fitted a *NB* model with the same terms, which was not
377 overdispersed (0.99, $P= 0.965$) and not zero-inflated (1.02, $P= 0.786$). Hence, we proceeded with
378 the *NB* distribution. While 24/145 males bred both in 2017 and 2018, we treated these breeding
379 events as independent after ascertaining that the residuals within these males were
380 uncorrelated in a null GLM *NB* model (Zuur *et al.* 2009, 2013). The covariates included were body
381 mass, tarsus and wing length, local male density, study area and ringing year, their interactions
382 with *F*, and *F*, mass, wing and tarsus square effects. All the models included the number of
383 encounters and ringing year (Table S2b).
384 (3) *Female inbreeding and clutch size*. This candidate set was constructed using linear models. As
385 covariates, we included the mother body mass, tarsus and wing length, and their quadratic
386 effects, breeding peak (present in each model as it strongly predicts the clutch size), sum of
387 rainfall during and mean daily temperature averaged for 15 days prior to start of incubation,
388 study area and year, and the interactions of all the covariates with mother *F*. We restricted the
389 number of non-intercept estimates in a model to 6 (Table S4a).
390 (4) *Female inbreeding and egg hatching success*. The hatching success was coded as 1 for eggs that
391 hatched and 0 otherwise, with the egg being the subject. The candidate set was built using
392 generalized linear mixed models (GLMMs) with package *lme4* (Bates *et al.* 2015) and the
393 binomial distribution with logit link. Nest ID was entered as a random factor. As covariates, we
394 included the breeding peak, sum of rainfall and mean average daily temperature during
395 incubation, clutch size, study area and year. Due to the low number of unhatched eggs ($N= 23$),
396 we limited the number of non-intercept estimates in a model to 2 and did not consider
397 interactions (Table S4b).
398 (5) *Female inbreeding and nestling survival*. The nestling survival was coded as 1 for nestlings that
399 survived until fledging and 0 otherwise, with the nestling being the subject. The candidate set
400 was constructed with GLMMs, as above. As covariates, we included the mother body mass, wing
401 and tarsus length, breeding peak, sum of rainfall and mean average daily temperature from
402 hatching to fledging, hatched brood size, study area and year. Due to the low number of nestling
403 deaths ($N= 22$), we limited the number of non-intercept estimates in a model to 2 and did not
404 consider interactions (Table S4c).
405 (6) *Female inbreeding and fledged brood size*. We considered only successful nests (i.e. those that
406 fledged at least 1 chick), as nests fail completely for reasons that are mostly independent of the

407 female (e.g. predation). The candidate set was built using linear models. As covariates, we
408 included the mother body mass, wing and tarsus length and their quadratic effects, breeding
409 peak, sum of rainfall and mean average daily temperature from hatching to fledging, study area
410 and year. We also considered interactions of the covariates with *F*. The number of non-intercept
411 estimates in a model was <8 (Table S4d).

412 (7) *Nestling inbreeding and tarsus length on days 2, 5 and 9 post-hatch*. In natural populations,
413 phenotype-associated inbreeding can occur, e.g. if the wing length of a parent is correlated with
414 its relatedness to the mate. This creates a bias on the inbreeding depression especially in
415 morphological traits, as part of variation in the trait results from genetic covariance with the
416 relatedness between parents. Therefore, as recommended by Becker *et al.* (2016), we applied
417 the animal model. We used package *MCMCglmm* (Hadfield 2010), with the random effects being
418 the breeding value ('animal'), chick ID, nest ID and father ID (from the Colony results). We
419 calculated the genomic relatedness matrix using package *AGHmatrix* (Amadeu *et al.* 2023) and
420 the Van Raden matrix. We applied an uninformative prior and set the number of MCMC
421 iterations to 1.2 million, burnin to 10000 and thinning to 100. The candidate set considered the
422 following covariates: measurement day (present in all models), chick sex, brood size, breeding
423 peak, sum of rainfall during the previous 14 days, mean average daily temperature over the
424 previous 4 days, prey abundance, area and year, and their interaction with chick *F*; and mother
425 *F*, to account for an effect of maternal inbreeding on brood provisioning and parent-offspring
426 correlation in *F* (Nietlisbach *et al.* 2016) (Table S6).

427

428 ## Results

429 *Parentage assignment and inbreeding statistics*

430 Of the 320 assignments, in further analysis we used 223 that were of ≥99% confidence in both the
431 father-offspring pair and trio (i.e. father-mother-offspring), and 2 that were of ≥99% confidence in
432 father-offspring pair, but their mother was not sampled and trio confidence could not be
433 determined. We excluded 1 assignment for which the trio confidence was 99%, but the pair
434 confidence was <95%. Of the 173 candidate fathers, 58 were assigned paternity with confidence as
435 above. The range and median number of mismatches were: 0-3 and 0 for mother-chick; 0-5 and 1 for
436 the 225 trios with the most likely father; and 0-49 and 39 for the 225 trios with the second most
437 likely father. We obtained same assignments with the strict and relaxed confidence of 80% and 95%,
438 respectively. All the Colony paternity assignments matched the 225 Cervus assignments and had the
439 probability of 1.

The mean ±SD *F* was 0.005 ±0.043, median 0.002 and range –0.077 to 0.138 for adult females; and mean ±SD 0.028 ±0.048, median 0.030 and range –0.101 to 0.168 for adult males (Fig. S3). Two nestlings with unusually low inbreeding coefficients were removed from the tarsus analysis as outliers. The mean ±SD offspring *F*, excluding these outliers, was 0.007 ±0.046, median 0.006 and range –0.096 to 0.175. The *g2* was estimated at 0.0009 (95% confidence interval 0.0002 to 0.0015) (Fig. S4). There was a moderate positive correlation between the mother *F* and the mean within-mother chick *F* (Pearson *r*= 0.30, 95% CI 0.05 to 0.52).

*Inbreeding depression on fitness components in adults*

In adult males, the return rate was predicted neither by the male *F* nor by the *F* by phenotype interactions, as the interaction models received weak support, and the CIs of these terms overlapped zero (Fig. 2, Tables 2a & 3a). The *F* and tarsus squared model obtained top support (ωAICc=0.28), was 8.8 times more likely than the *F* and tarsus model, and 3.5 times more likely than the null model. The *F* squared models were also well supported (sum of ωAICc= 0.47) but only weakly more probable compared to the null model (Table S2a). The inverse quadratic relationships with the tarsus and *F* indicated that return rates are the highest for males with average tarsi and *F* values, respectively.

While the male *F* was not a good predictor of the breeding success for average phenotypes and male densities (Fig. 2, Table S3b), the *F* by tarsus interaction model scored the highest (ωAICc=0.47), was 4.9 times more probable than the null model and 16.7 times more probable than the *F* and tarsus model (Table S2b). The remaining interaction effects obtained low support. In males with small tarsi, the *F* estimate was negative, and in males with exceptionally large tarsi it was positive, however, the latter result was based on very few observations and thus uncertain (Fig. 3).

For average covariates, the female *F* relationship with the clutch size was unsupported (Fig. 4, Table S5a). However, the *F* by tarsus interaction model obtained top support (ωAICc=0.52), was 4.3 times more probable than the *F* and tarsus model, and clearly more parsimonious than the null model (Table S4a). The remaining interaction effects were unsupported. In females with small tarsi, the *F* effect on the clutch size was negative, while in those with the largest tarsi it appeared positive; however, the latter result was based on very few observations and thus uncertain (Fig. 5). The tarsus models ranked the highest (sum of ωAICc 0.99), pointing to the tarsus as the strongest and positive predictor of the clutch size (Fig. 4, Tables S4a&S5a).

Mother *F* showed no clear relationship with the hatching success and nestling survival (Fig. 4, Tables S5b-c). For the hatching success, the null model scored the highest (ωAICc=0.21) and support was spread between several models (Table S4b). For the nestling survival, the *F* and body mass model obtained clear support from the data (ωAICc=0.70) (Table S4c), showing that mother body mass was a strong negative correlate of nestling survival (Fig. 4, Table S5c).

Similarly, the relationship between the mother *F* and fledged brood size was not supported for average phenotypic and environmental covariates (Fig. 4, Table S5d). The null model ranked the second and the *F* by body mass interaction model was 4.4 times more probable than the *F* and body mass model, however, it was nearly as parsimonious as the null model, indicating very low support (Table S4d). The remaining interaction effects were not supported. The breeding peak was a relatively strong predictor of the fledged broood size (Fig. 4, Table S5d).

*Inbreeding depression on nestling tarsus*

The 95% credible interval of the model-averaged chick *F* effect spanned zero, indicating no support for an association between *F* and tarsus for average covariates (Table S7). Evidence was spread between several animal models (Table S6). The *F* by rainfall and *F* by temperature interaction models scored best (ωDIC=0.12 and 0.11, respectively). The *F* by temperature interaction estimate was negative, suggesting that the *F* effect becomes more negative with increasing temperatures and varies by year. We obtained low evidence for the remaining interactions (Tables S6 & S7).

*Inbreeding load and change in fitness*

For average phenotypic traits, the inbreeding load on male return rates was moderate, with nearly half the number of years returned to the breeding grounds in the most inbred males, compared to the least inbred ones, and the inbreeding load on the male breeding success was high (Table 1). However, as the 95% CIs of the male *F* effects spanned zero, these inbreeding load estimates bear high uncertainty. The males with average small tarsi incurred strong inbreeding load, with almost 90% reduction in the number of young for the most inbred males, compared to the least inbred ones. In contrast, in males with average large tarsi the inbreeding load was negligible (Table 1).

The female inbreeding load on the clutch size was low for the average covariates. However, mothers with average small tarsi bore higher, although moderate inbreeding load, with about 10% reduction in the clutch size for the most inbred relative to the least inbred females, while in mothers

502 with average large tarsi the inbreeding load was very low (Table 1). The mother inbreeding load on
503 the hatching success, nestling survival and fledged brood size was also low. The overall decrease in
504 fitness between laying a clutch and brood fledging totalled 0.6 haploid lethal equivalents (Table 1).

505

506 ## Discussion

507 *Weak inbreeding depression for average phenotypic and environmental variables*

508 For the mean value of the phenotypic traits and male density in the case of the breeding success,
509 inbreeding depression on the long-term return rates and seasonal breeding success of adult males
510 obtained low support from the data. Male aquatic warblers show high post-breeding annual return
511 rates (Dyrcz & Zdunek 1993, Bellebaum 2018), which are comparable to survival rates of other
512 migratory passerines in the central European latitude (Scholer *et al.* 2020). Hence, the 4-year return
513 rate is a strong predictor for the lifespan survival. Given the median return rate of 1 year among the
514 surviving males, most males reproduce over 1 breeding season, indicating that the seasonal
515 breeding success is a proxy for the lifetime reproductive success. Therefore, our results do not
516 suggest that the inbreeding rate in adult males is associated with their adult lifespan nor the lifetime
517 reproductive success.

518 Avian studies on the inbreeding depression on adult survival have been scarce and showed
519 weak, e.g. $B$= 1.7 (Keller 1998), moderate, e.g. $\delta$= 49% (Harrisson *et al.* 2019) or strong effects of
520 inbreeding, e.g. up to $B$= 7 in the house sparrow (*Passer domesticus*) (Niskanen *et al.* 2020). Evidence
521 for male inbreeding effects on the annual reproductive success has also been variable, ranging from
522 weak support (Sin *et al.* 2021), through moderate effects, e.g. $\delta$= 42% (Harrisson *et al.* 2019) to
523 clearly negative inbreeding depression in the house sparrow, $B$= 6 (Niskanen *et al.* 2020). The $B$= 4.9
524 and $\delta$= 69% that we obtained for aquatic warbler males appear to be high inbreeding load on the
525 annual reproductive success, however, these estimates bear high uncertainty.

526 Similarly to males, for the mean value of the phenotypic and environmental covariates, we
527 found weak support for the relationship between an adult female's inbreeding rate and her short-
528 term fitness components. These results do not support mother inbreeding depression on offspring
529 production from clutch laying until fledging in the aquatic warbler. However, it is the earliest
530 developmental stages that could respond more negatively to inbreeding (Noordwijk & Scharloo
531 1981, Hemmings *et al.* 2012b), and it is inbreeding of the offspring that could affect its survival more
532 strongly.

533 Previous studies on birds found the parental inbreeding to be little related to egg production
534 (Keller 1998, Szulkin *et al.* 2007, Harrisson *et al.* 2019). In the takahe (*Porphyrio hochstetteri*),
535 parental inbreeding was unassociated with hatching rates ($B$= –0.7) and fledging success ($B$= 3.3)
536 (Grueber *et al.* 2010), but in another study the latter decreased by 30% in mothers with the pedigree
537 $f>0$ (Jamieson *et al.* 2003). Negative effects of maternal inbreeding were demonstrated in two
538 studies on passerine birds for the hatching success ($\delta$= 20-36%) and fledgling production ($\delta$= 26%)
539 (Keller 1998, Harrisson *et al.* 2019). In our study, although the clutch size manifested the highest
540 inbreeding load of the female fitness components studied, it was relatively low, and so was the
541 inbreeding load from clutch laying to brood fledging.

542 Neither did we find unambiguous evidence that, for average values of the phenotypic and
543 environmental covariates, and while accounting for mother inbreeding, the offspring inbreeding rate
544 is associated with the tarsus length, and this association remained constant across the three nestling
545 ages. This does not support inbreeding depression on the skeletal body size in aquatic warbler
546 nestlings, for typical individuals and conditions. In contrast, in the collared flycatcher (*Ficedula*
547 *albicollis*), inbred fledglings had smaller tarsi compared to outbred ones (Kruuk *et al.* 2002), but no
548 such relationship was found in another species (Sin *et al.* 2021).

549

550 *Effects of inbreeding depend on body size in adults and on weather in offspring*

551 We demonstrated that inbreeding depression on the male seasonal breeding success and clutch size
552 is conditional on the tarsus length of males and females, respectively. In birds, tarsus length is a
553 proxy for the structural body size (Rising & Somers 1989, Senar & Pascual 1997), implying that the
554 inbreeding costs on these fitness-related traits increase in small-bodied individuals, relative to large-
555 bodied individuals. In some passerines, the tarsus or a body size index is positively associated with
556 the clutch size in females (Alatalo & Lundberg 1986, Sedinger *et al.* 1995, Garamszegi *et al.* 2004, this
557 study) and with sperm quality and functionality traits and testis size in males (Brown & Brown 2003,
558 Forstmeier *et al.* 2017), which translates into sperm production (Parker & Pizzari 2010, Hayward &
559 Gillooly 2011). Therefore, it could be more difficult for small inbred individuals to compensate for
560 their lower fecundity traits, than it is for large inbred ones.

561 The inbreeding depression on the breeding success in the small-bodied males appears
562 strong. For example, the $B$ of 9 and ~89% decrease in the male annual reproductive success are
563 comparable to the high inbreeding depression in the house sparrow (Niskanen *et al.* 2020). In small-
564 bodied females, the inbreeding load on clutch sizes ($B$= 2.8) and the decrease in the clutch size
565 produced (~11%) were moderate and did not translate to decreased fledgling production. Our

finding of inbreeding depression on the clutch size in small females stands in contrast with previous studies (Keller 1998, Szulkin *et al.* 2007, Harrisson *et al.* 2019).

We did not obtain firm support for environmental dependence of the chick inbreeding effects on tarsus, except for a weak interaction with the average daily temperature. This interaction suggests that chick *F* was more negatively associated with the tarsus in higher temperatures in the preceding days. As temperature was standardised within year, breeding peak and day, its effect was independent of these factors. Elevated temperatures could correlate with lower abundance or availability of prey, and thus more inbred chicks could cope worse with being fed less during warmer days. As the effect of nestling *F* varied between the two study years, the magnitude and direction of inbreeding effects on nestling body size could differ between breeding seasons.

*Conclusions and conservation implications*

We sought to determine the magnitude of the inbreeding depression on fitness components and nestling growth in a threatened passerine, the aquatic warbler, and to inspect whether the inbreeding effects on these traits are modulated by the phenotype and environment. We demonstrated, to our knowledge for the first time, that in birds, inbreeding depression on adult fitness components could depend on the body size, with smaller individuals paying higher costs of inbreeding. This suggests that birds raised in poor environmental conditions, which negatively affect the adult body size (De Kogel 1997, Searcy *et al.* 2004, Cleasby *et al.* 2011) could have lower fitness if they are inbred. Our study also points out that accounting for the body size (and possibly other phenotypic and environmental variables) allows to determine inbreeding depression more precisely. This is of considerable importance especially in the case of species of conservation concern, where nuanced knowledge on inbreeding depression will be informative for adequate estimation of extinction risk. Finally, our observation that nestling inbreeding association with tarsus is conditioned by the temperature and year partly corroborates that unfavourable environmental conditions could exacerbate inbreeding depression. It also implies that survival to reproductive maturity, of which the chick tarsus length is a proxy, could be negatively affected for nestlings growing in excessively warm ambient temperatures.

For the aquatic warbler, our study shows that for average phenotypic and environmental covariates, inbreeding effects on the studied fitness traits are weakly supported. However, we were able to estimate inbreeding depression on fitness traits only in adults. Weakly negative inbreeding effects on short-term fitness components can accumulate to high inbreeding load over the complete

life history continuum (Szulkin *et al.* 2007, Grueber *et al.* 2010, Harrisson *et al.* 2019, Niskanen *et al.* 2020). Future studies on the inbreeding depression in the aquatic warbler should include the missing fitness components, e.g. survival from viable egg to sexual maturity, juvenile survival and adult female survival. Notwithstanding, our results will be informative for a population viability analysis accounting for inbreeding depression (O'Grady *et al.* 2006, Nonaka *et al.* 2019) and for conservation actions such as translocation.

## References


**Alatalo, R. V & Lundberg, A.** 1986. Heritability and selection on tarsus length in the pied flycatcher (*Ficedula hypoleuca*). *Evolution* **40**: 574–583.

**Amadeu, R.R., Garcia, A.A.F., Munoz, P.R. & Ferrão, L.F. V**. 2023. AGHmatrix: genetic relationship matrices in R. *Bioinformatics* **39**: btad445.

**Andrews, K.R., Adams, J.R., Cassirer, E.F., Plowright, R.K., Gardner, C., Dwire, M., Hohenlohe, P.A. & Waits, L.P.** 2018. A bioinformatic pipeline for identifying informative SNP panels for parentage assignment from RADseq data. *Mol. Ecol. Resour.* **18**: 1263–1281.

**Armbruster, P. & Reed, D.H.** 2005. Inbreeding depression in benign and stressful environments. *Heredity* **95**: 235–242.

**Balloux, F., Amos, W. & Coulson, T.** 2004. Does heterozygosity estimate inbreeding in real populations? *Mol. Ecol.* **13**: 3021–3031.

**Bartoń, K.** 2019. MuMIn: Multi-Model Inference. R package version 1.43.6.

**Bates, D., Mächler, M., Bolker, B. & Walker, S.** 2015. Fitting linear mixed-effects models using lme4. *J. Stat. Softw.* **67**: 1–48.

**Bayona-Vásquez, N.J., Glenn, T.C., Kieran, T.J., Pierson, T.W., Hoffberg, S.L., Scott, P.A., Bentley, K.E., Finger, J.W., Louha, S., Troendle, N., Diaz-Jaimes, P., Mauricio, R. & Faircloth, B.C.** 2019. Adapterama III: Quadruple-indexed, double/triple-enzyme RADseq libraries (2RAD/3RAD). *PeerJ* **7**: e7724.

**Becker, P.J.J., Hegelbach, J., Keller, L.F. & Postma, E.** 2016. Phenotype-associated inbreeding biases estimates of inbreeding depression in a wild bird population. *J. Evol. Biol.* **29**: 35–46.

**Bellebaum, J.** 2018. Population dynamics. In: *The Aquatic Warbler conservation handbook* (F. Tanneberger & J. Kubacka, eds), pp. 68–71. Brandenburg State Office for Environment (LfU), Potsdam, Germany.

**Bolger, A.M., Lohse, M. & Usadel, B.** 2014. Trimmomatic: a flexible trimmer for Illumina sequence data. *Bioinformatics* **30**: 2114–2120.

**Briedis, M. & Keišs, O.** 2016. Extracting historical population trends using archival ringing data - an example: the globally threatened Aquatic Warbler. *J. Ornithol.* **157**: 419–425.

**Brook, B.W., Tonkyn, D.W., O'Grady, J.J. & Frankham, R.** 2002. Contribution of inbreeding to extinction risk in threatened species. *Ecol. Soc.* **6**: 16.

**Brown, C.R. & Brown, M.B.** 2003. Testis size increases with colony size in cliff swallows. *Behav. Ecol.*

**14**: 569–575.

**Burnham, K.P. & Anderson, D.R.** 2002. *Model selection and multimodel inference: A practical information-theoretic approach*, 2nd ed. Springer-Verlag, New York, USA.

**Catchen, J., Hohenlohe, P.A., Bassham, S., Amores, A. & Cresko, W.A.** 2013. Stacks: An analysis tool set for population genomics. *Mol. Ecol.* **22**: 3124–3140.

**Catchen, J.M., Amores, A., Hohenlohe, P., Cresko, W. & Postlethwait, J.H.** 2011. Stacks: Building and genotyping loci de novo from short-read sequences. *G3 Genes|Genomes|Genetics* **1**: 171–182.

**Cleasby, I.R., Burke, T., Schroeder, J. & Nakagawa, S.** 2011. Food supplements increase adult tarsus length, but not growth rate, in an island population of house sparrows (Passer domesticus). *BMC Res. Notes* **4**: 431.

**Crnokrak, P. & Roff, D.A.** 1999. Inbreeding depression in the wild. *Heredity* **83**: 260–270.

**Danecek, P., Auton, A., Abecasis, G., Albers, C.A., Banks, E., DePristo, M.A., Handsaker, R.E., Lunter, G., Marth, G.T., Sherry, S.T., McVean, G., Durbin, R. & Group, 1000 Genomes Project Analysis**. 2011. The variant call format and VCFtools. *Bioinformatics* **27**: 2156–2158.

**Danecek, P., Bonfield, J.K., Liddle, J., Marshall, J., Ohan, V., Pollard, M.O., Whitwham, A., Keane, T., McCarthy, S.A., Davies, R.M. & Li, H.** 2021. Twelve years of SAMtools and BCFtools. *Gigascience* **10**: giab008.

**David, P., Pujol, B., Viard, F., Castella, V. & Goudet, J.** 2007. Reliable selfing rate estimates from imperfect population genetic data. *Mol. Ecol.* **16**: 2474–2487.

**De Kogel, C.H.** 1997. Long-Term Effects of Brood Size Manipulation on Morphological Development and Sex-Specific Mortality of Offspring. *J. Anim. Ecol.* **66**: 167–178.

**De Meeûs, T.** 2018. Revisiting FIS, FST, Wahlund Effects, and Null Alleles. *J. Hered.* **109**: 446–456.

**Dodt, M., Roehr, J.T., Ahmed, R. & Dieterich, C.** 2012. FLEXBAR-Flexible Barcode and Adapter Processing for Next-Generation Sequencing Platforms. *Biology (Basel).* **1**: 895–905.

**Driller, M., Arantes, L.S., Vilaça, S.T., Carrasco-Valenzuela, T., Heeger, F., Mbedi, S., Chevallier, D., De Thoisy, B. & Mazzoni, C.J.** 2021. Achieving high-quality ddRAD-like reference catalogs for non-model species: the power of overlapping paired-end reads. *bioRxiv* 2020.04.03.024331.

**Dyrcz, A., Wink, M., Backhaus, A., Zdunek, W., Leisler, B. & Schulze-Hagen, K.** 2002. Correlates of multiple paternity in the Aquatic Warbler (*Acrocephalus paludicola*). *J. Ornithol.* **143**: 430–439.

**Dyrcz, A., Wink, M., Kruszewicz, A. & Leisler, B.** 2005. Male reproductive success is correlated with blood parasite levels and body condition in the promiscuous Aquatic Warbler (*Acrocephalus paludicola*). *Auk* **122**: 558–565.

**Dyrcz, A. & Zdunek, W.** 1993. Breeding ecology of the Aquatic Warbler *Acrocephalus paludicola* on the Biebrza marshes, northeast Poland. *Ibis* **135**: 181–189.

**Evans, S.R. & Sheldon, B.C.** 2008. Interspecific patterns of genetic diversity in birds: correlations with extinction risk. *Conserv. Biol.* **22**: 1016–1025.

**Faux, P., Oliveira, J.C.P., Campos, D.P., Dantas, G.P.M., Maia, T.A., Dergan, C.G., Cassemiro, P.M., Hajdu, G.L., Santos-Júnior, J.E. & Santos, F.R.** 2020. Fast genomic analysis of aquatic bird populations from short single-end reads considering sex-related pitfalls. *Ecol. Inform.* **56**: 101058.

677 **Flade, M., Malashevich, U., Krogulec, J., Poluda, A., Preiksa, Z., Végvári, Z. & Lachmann, L.** 2018.
678 World distribution, population, and trends. In: *The Aquatic Warbler conservation handbook* (F.
679 Tanneberger & J. Kubacka, eds), pp. 22–35. Brandenburg State Office for Environment (LfU),
680 Potsdam, Germany.

681 **Flanagan, S.P. & Jones, A.G.** 2019. The future of parentage analysis: From microsatellites to SNPs
682 and beyond. *Mol. Ecol.* **28**: 544–567.

683 **Forstmeier, W., Ihle, M., Opatová, P., Martin, K., Knief, U., Albrechtová, J., Albrecht, T. &**
684 **Kempenaers, B.** 2017. Testing the phenotype-linked fertility hypothesis in the presence and
685 absence of inbreeding. *J. Evol. Biol.* **30**: 968–976.

686 **Fox, C.W. & Reed, D.** 2010. Inbreeding depression increases with maternal age in a seed-feeding
687 beetle. *Evol. Ecol. Res.* **12**: 961–972.

688 **Gage, M.J.G., Surridge, A.K., Tomkins, J.L., Green, E., Wiskin, L., Bell, D.J. & Hewitt, G.M.** 2006.
689 Reduced heterozygosity depresses sperm quality in wild rabbits, Oryctolagus cuniculus. *Curr.*
690 *Biol.* **16**: 612–617.

691 **Garamszegi, L.Z., Török, J., Tóth, L. & Michl, G.** 2004. Effect of timing and female quality on clutch
692 size in the Collared Flycatcher Ficedula albicollis . *Bird Study* **51**: 270–277.

693 **Gebhardt-Henrich, S. & Richner, H.** 1998. Causes of Growth Variation and Its Consequences for
694 Fitness.

695 **Glenn, T.C., Nilsen, R.A., Kieran, T.J., Sanders, J.G., Bayona-Vásquez, N.J., Finger, J.W., Pierson,**
696 **T.W., Bentley, K.E., Hoffberg, S.L., Louha, S., Garcia-De Leon, F.J., Del Rio Portilla, M.A., Reed,**
697 **K.D., Anderson, J.L., Meece, J.K., Aggrey, S.E., Rekaya, R., Alabady, M., Belanger, M., Winker,**
698 **K. & Faircloth, B.C.** 2019. Adapterama I: universal stubs and primers for 384 unique dual-
699 indexed or 147,456 combinatorially-indexed Illumina libraries (iTru & iNext). *PeerJ* **7**: e7755.

700 **Gruber, B., Unmack, P.J., Berry, O.F. & Georges, A.** 2018. dartR: An R package to facilitate analysis of
701 SNP data generated from reduced representation genome sequencing. *Mol. Ecol. Resour.* **18**:
702 691–699.

703 **Grueber, C.E., Laws, R.J., Nakagawa, S. & Jamieson, I.G.** 2010. Inbreeding depression accumulation
704 across life-history stages of the endangered takahe. *Conserv. Biol.* **24**: 1617–1625.

705 **Grueber, C.E., Nakagawa, S., Laws, R.J. & Jamieson, I.G.** 2011. Multimodel inference in ecology and
706 evolution: challenges and solutions. *J. Evol. Biol.* **24**: 699–711.

707 **Hadfield, J.D.** 2010. MCMC Methods for Multi-Response Generalized Linear Mixed Models: The
708 {MCMCglmm} {R} Package. *J. Stat. Softw.* **33**: 1–22.

709 **Harrell, F.E.** 2015. Multivariable Modeling Strategies BT - Regression Modeling Strategies: With
710 Applications to Linear Models, Logistic and Ordinal Regression, and Survival Analysis. In: (J.
711 Harrell Frank E., ed), pp. 63–102. Springer International Publishing, Cham.

712 **Harrisson, K.A., Magrath, M.J.L., Yen, J.D.L., Pavlova, A., Murray, N., Quin, B., Menkhorst, P.,**
713 **Miller, K.A., Cartwright, K. & Sunnucks, P.** 2019. Lifetime Fitness Costs of Inbreeding and Being
714 Inbred in a Critically Endangered Bird. *Curr. Biol.* **29**: 2711-2717.e4.

715 **Hartig, F.** 2022. DHARMa: Residual Diagnostics for Hierarchical (Multi-Level / Mixed) Regression
716 Models.

717 **Hayward, A. & Gillooly, J.F.** 2011. The Cost of Sex: Quantifying Energetic Investment in Gamete
718 Production by Males and Females. *PLoS One* **6**: e16557.

**Hemmings, N., West, M. & Birkhead, T.R.** 2012a. Causes of hatching failure in endangered birds. *Biol. Lett.* **8**: 964–967.

**Hemmings, N.L., Slate, J. & Birkhead, T.R.** 2012b. Inbreeding causes early death in a passerine bird. *Nat. Commun.* **3**: 863.

**Hinkson, K.M. & Poo, S.** 2020. Inbreeding depression in sperm quality in a critically endangered amphibian. *Zoo Biol.* **39**: 197–204.

**Hoffberg, S.L., Kieran, T.J., Catchen, J.M., Devault, A., Faircloth, B.C., Mauricio, R. & Glenn, T.C.** 2016. RADcap: sequence capture of dual-digest RADseq libraries with identifiable duplicates and reduced missing data. *Mol. Ecol. Resour.* **16**: 1264–1278.

**Huisman, J.** 2017. Pedigree reconstruction from SNP data: parentage assignment, sibship clustering and beyond. *Mol. Ecol. Resour.* **17**: 1009–1024.

**Huisman, J., Kruuk, L.E.B., Ellis, P.A., Clutton-Brock, T. & Pemberton, J.M.** 2016. Inbreeding depression across the lifespan in a wild mammal population. *Proc. Natl. Acad. Sci.* **113**: 3585–3590.

**Jamieson, I.G., Roy, M.S. & Lettink, M.** 2003. Sex-Specific Consequences of Recent Inbreeding in an Ancestrally Inbred Population of New Zealand Takahe. *Conserv. Biol.* **17**: 708–716.

**Jones, O.R. & Wang, J.** 2010. COLONY: a program for parentage and sibship inference from multilocus genotype data. *Mol. Ecol. Resour.* **10**: 551–555.

**Kalinowski, S.T., Taper, M.L. & Marshall, T.C.** 2007. Revising how the computer program Cervus accommodates genotyping error increases success in paternity assignment. *Mol. Ecol.* **16**: 1099–1106.

**Kardos, M., Luikart, G. & Allendorf, F.W.** 2015. Measuring individual inbreeding in the age of genomics: marker-based measures are better than pedigrees. *Heredity* **115**: 63–72.

**Keller, L.F.** 1998. Inbreeding and Its Fitness Effects in an Insular Population of Song Sparrows (Melospiza melodia). *Evolution* **52**: 240–250.

**Keller, L.F., Grant, P.R., Grant, B.R. & Petren, K.** 2002. Environmental conditions affect the magnitude of inbreeding depression in survival of Darwin's finches. *Evolution* **56**: 1229–1239.

**Keller, L.F. & Waller, D.M.** 2002. Inbreeding effects in wild populations. *Trends Ecol. Evol.* **17**: 230–241.

**Kennedy, E.S., Grueber, C.E., Duncan, R.P. & Jamieson, I.G.** 2014. SEVERE INBREEDING DEPRESSION AND NO EVIDENCE OF PURGING IN AN EXTREMELY INBRED WILD SPECIES—THE CHATHAM ISLAND BLACK ROBIN. *Evolution* **68**: 987–995.

**Kruuk, L.E.B., Sheldon, B.C. & Merilä, J.** 2002. Severe inbreeding depression in collared flycatchers (Ficedula albicollis). *Proceedings. Biol. Sci.* **269**: 1581–1589.

**Kubacka, J., Dubiec, A., Korb, J., Salewski, V., Dyrcz, A., Foucher, J., Giessing, B., Leisler, B., Schulze-Hagen, K., Wink, M. & Panagiotopoulou, H.** 2024. Low genetic diversity and high gene flow in the Aquatic Warbler (*Acrocephalus paludicola*), a threatened marshland songbird with a fragmented breeding range. *Ibis* **166**: 232–251.

**Kubacka, J., Dubiec, A., Souza Arantes, L., Herdegen-Radwan, M., Mazzoni, C.J., Sparmann, S. & Osiejuk, T.S.** 2025. Agonistic song rate positively correlates with male breeding success and avian malaria infection in *Acrocephalus paludicola* (Aquatic Warbler), a promiscuous songbird with female-only parental care. *Ornithology* **142**: ukae045.

**Kubacka, J., Oppel, S., Dyrcz, A., Lachmann, L., Barros Da Costa, J.P.D., Kail, U. & Zdunek, W.** 2014. Effect of mowing on productivity in the endangered Aquatic Warbler *Acrocephalus paludicola. Bird Conserv. Int.* **24**: 45–58.

**Langmead, B., Trapnell, C., Pop, M. & Salzberg, S.L.** 2009. Ultrafast and memory-efficient alignment of short DNA sequences to the human genome. *Genome Biol.* **10**: R25.

**Le Nevé, A., Blaize, C., Dehorter, O., Dugué, H., Hemery, D., Jiguet, F., Musseau, R., Neto, J.M., Rguibi Idrissi, H., Zumalacárregui Martínez, C. & Roothaert, N.** 2018. Migration. In: *The Aquatic Warbler conservation handbook* (F. Tanneberger & J. Kubacka, eds), pp. 72–89. Brandenburg State Office for Environment (LfU), Potsdam, Germany.

**Leisler, B. & Schulze-Hagen, K.** 2011. Reed warblers reproduced. In: *The Reed Warblers. Diversity in a uniform family*, pp. 138–159. KNNV Publishing, Zeist, the Netherlands.

**Martin, M.** 2011. Cutadapt removes adapter sequences from high-throughput sequencing reads. *EMBnet.journal; Vol 17, No 1 Next Gener. Seq. Data Anal.*, doi: 10.14806/ej.17.1.200.

**Matthews, T.J., Cottee-Jones, H.E. & Whittaker, R.J.** 2014. Habitat fragmentation and the species–area relationship: a focus on total species richness obscures the impact of habitat loss on habitat specialists. *Divers. Distrib.* **20**: 1136–1146.

**Mazerolle, M.J.** 2023. AICcmodavg: Model selection and multimodel inference based on (Q)AIC(c).

**Morton, N.E. & Crow, J.F.** 1956. An Estimate of the Mutational Damage in Man from Data on Consanguineous Marriages. *Proc. Natl. Acad. Sci. U. S. A.* **42**: 855–863.

**Nietlisbach, P., Keller, L.F. & Postma, E.** 2016. Genetic variance components and heritability of multiallelic heterozygosity under inbreeding. *Heredity* **116**: 1–11.

**Nietlisbach, P., Muff, S., Reid, J.M., Whitlock, M.C. & Keller, L.F.** 2019. Nonequivalent lethal equivalents: Models and inbreeding metrics for unbiased estimation of inbreeding load. *Evol. Appl.* **12**: 266–279.

**Niskanen, A.K., Billing, A.M., Holand, H., Hagen, I.J., Araya-Ajoy, Y.G., Husby, A., Rønning, B., Myhre, A.M., Ranke, P.S., Kvalnes, T., Pärn, H., Ringsby, T.H., Lien, S., Sæther, B.-E., Muff, S. & Jensen, H.** 2020. Consistent scaling of inbreeding depression in space and time in a house sparrow metapopulation. *Proc. Natl. Acad. Sci.* **117**: 14584–14592.

**Nonaka, E., Sirén, J., Somervuo, P., Ruokolainen, L., Ovaskainen, O. & Hanski, I.** 2019. Scaling up the effects of inbreeding depression from individuals to metapopulations. *J. Anim. Ecol.* **88**: 1202–1214.

**Noordwijk, A.J. Van & Scharloo, W.** 1981. Inbreeding in an Island Population of the Great Tit. *Evolution* **35**: 674–688.

**Nowak, C., Jost, D., Vogt, C., Oetken, M., Schwenk, K. & Oehlmann, J.** 2007. Consequences of inbreeding and reduced genetic variation on tolerance to cadmium stress in the midge Chironomus riparius. *Aquat. Toxicol.* **85**: 278–284.

**O'Grady, J.J., Brook, B.W., Reed, D.H., Ballou, J.D., Tonkyn, D.W. & Frankham, R.** 2006. Realistic levels of inbreeding depression strongly affect extinction risk in wild populations. *Biol. Conserv.* **133**: 42–51.

**Parker, G.A. & Pizzari, T.** 2010. Sperm competition and ejaculate economics. *Biol. Rev.* **85**: 897–934.

**Pflüger, F.J., Signer, J. & Balkenhol, N.** 2019. Habitat loss causes non-linear genetic erosion in specialist species. *Glob. Ecol. Conserv.* **17**: e00507.

**QGIS Development Team**. 2020. QGIS Geographic Information System. Open Source Geospatial Foundation Project.

**R Core Team**. 2024. R: A Language and Environment for Statistical Computing.

**Ralls, K., Ballou, J.D. & Templeton, A.** 1988. Estimates of Lethal Equivalents and the Cost of Inbreeding in Mammals. *Conserv. Biol.* **2**: 185–193.

**Rising, J.D. & Somers, K.M.** 1989. The Measurement of Overall Body Size in Birds. *Auk* **106**: 666–674.

**Rochette, N.C. & Catchen, J.M.** 2017. Deriving genotypes from RAD-seq short-read data using Stacks. *Nat. Protoc.* **12**: 2640–2659.

**Scholer, M.N., Strimas-Mackey, M. & Jankowski, J.E.** 2020. A meta-analysis of global avian survival across species and latitude. *Ecol. Lett.* **23**: 1537–1549.

**Schulze-Hagen, K., Flinks, H. & Dyrcz, A.** 1989. Brutzeitliche Beutewahl beim Seggenrohrsänger *Acrocephalus paludicola*. *J. Ornithol.* **130**: 251–255.

**Searcy, W.A., Peters, S. & Nowicki, S.** 2004. Effects of early nutrition on growth rate and adult size in song sparrows Melospiza melodia. *J. Avian Biol.* **35**: 269–279.

**Sedinger, J.S., Flint, P.L. & Lindberg, M.S.** 1995. Environmental Influence on Life-History Traits: Growth, Survival, and Fecundity in Black Brant (Branta Bernicla). *Ecology* **76**: 2404–2414.

**Senar, J.C. & Pascual, J.** 1997. Keel and tarsus length may provide a good predictor of avian body size. *Ardea* **85**.

**Sin, S.Y.W., Hoover, B.A., Nevitt, G.A. & Edwards, S. V**. 2021. Demographic History, Not Mating System, Explains Signatures of Inbreeding and Inbreeding Depression in a Large Outbred Population. *Am. Nat.* **197**: 658–676.

**Stoffel, M.A., Esser, M., Kardos, M., Humble, E., Nichols, H., David, P. & Hoffman, J.I.** 2016. inbreedR: an R package for the analysis of inbreeding based on genetic markers. *Methods Ecol. Evol.* **7**: 1331–1339.

**Symonds, M.R.E. & Moussalli, A.** 2011. A brief guide to model selection, multimodel inference and model averaging in behavioural ecology using Akaike's information criterion. *Behav. Ecol. Sociobiol.* **65**: 13–21.

**Szulkin, M., Bierne, N. & David, P.** 2010. Heterozygosity-fitness correlations: a time for reappraisal. *Evolution* **64**: 1202–1217.

**Szulkin, M., Garant, D., McCleery, R.H. & Sheldon, B.C.** 2007. Inbreeding depression along a life-history continuum in the great tit. *J. Evol. Biol.* **20**: 1531–1543.

**Szulkin, M. & Sheldon, B.C.** 2007. The Environmental Dependence of Inbreeding Depression in a Wild Bird Population. *PLoS One* **2**: e1027.

**Tanneberger, F., Alexander, K., Poluda, A., Bellebaum, J., Lachmann, L. & Flade, M.** 2018a. Threats and limiting factors. In: *The Aquatic Warbler conservation handbook* (F. Tanneberger & J. Kubacka, eds), pp. 106–121. Brandenburg State Office for Environment (LfU), Potsdam, Germany.

**Tanneberger, F., Kloskowski, J., Knöfler, V., Kozulin, A., Marczakiewicz, Piotr Morkvėnas, Ž., Poluda, A., Végvári, Z., Vergeichik, L. & Flade, M.** 2018b. Breeding habitat requirements. In: *The Aquatic Warbler conservation handbook* (F. Tanneberger & J. Kubacka, eds), pp. 34–45. Brandenburg State Office for Environment (LfU), Potsdam, Germany.

**Thrasher, D.J., Butcher, B.G., Campagna, L., Webster, M.S. & Lovette, I.J.** 2018. Double-digest RAD sequencing outperforms microsatellite loci at assigning paternity and estimating relatedness: A proof of concept in a highly promiscuous bird. *Mol. Ecol. Resour.* **18**: 953– 965.

**Venables, W.N. & Ripley, B.D.** 2002. *Modern Applied Statistics with S*, Fourth. Springer, New York.

**Vitorino, L.C., Borges Souza, U.J., Jardim, T.P.F.A. & Ballesteros–mejia, L.** 2019. Towards inclusion of genetic diversity measures into IUCN assessments: a case study on birds. *Anim. Biodivers. Conserv.* **42.2**: 317–335.

**Wang, J.** 2014. Marker-based estimates of relatedness and inbreeding coefficients: an assessment of current methods. *J. Evol. Biol.* **27**: 518–530.

**Waples, R.S.** 2015. Testing for Hardy–Weinberg Proportions: Have We Lost the Plot? *J. Hered.* **106**: 1–19.

**Westemeier, R.L., Brawn, J.D., Simpson, S.A., Esker, T.L., Jansen, R.W., Walk, J.W., Kershner, E.L., Bouzat, J.L. & Paige, K.N.** 1998. Tracking the long-term decline and recovery of an isolated population. *Science* **282**: 1695–1698.

**Wickham, H.** 2016. *ggplot2: Elegant Graphics for Data Analysis.* Springer-Verlag New York.

**Zhang, J., Kobert, K., Flouri, T. & Stamatakis, A.** 2014. PEAR: a fast and accurate Illumina Paired-End reAd mergeR. *Bioinformatics* **30**: 614–620.

**Zuur, A.F., Hilbe, J.M. & Ieno, E.N.** 2013. *A Beginner's Guide to GLM and GLMM with R*. Highland Statistics Ltd., Newburgh, United Kingdom.

**Zuur, A.F. & Ieno, E.N.** 2021. *The World of Zero-Inflated Models. Volume 1: Using GLM*. Highland Statistics Ltd., Newburgh, United Kingdom.

**Zuur, A.F., Ieno, E.N., Walker, N., Saveliev, A.A. & Smith, G.M.** 2009. *Mixed Effects Models and Extensions in Ecology with R*, 1st ed. Springer New York, New York, USA.

## Figures and tables

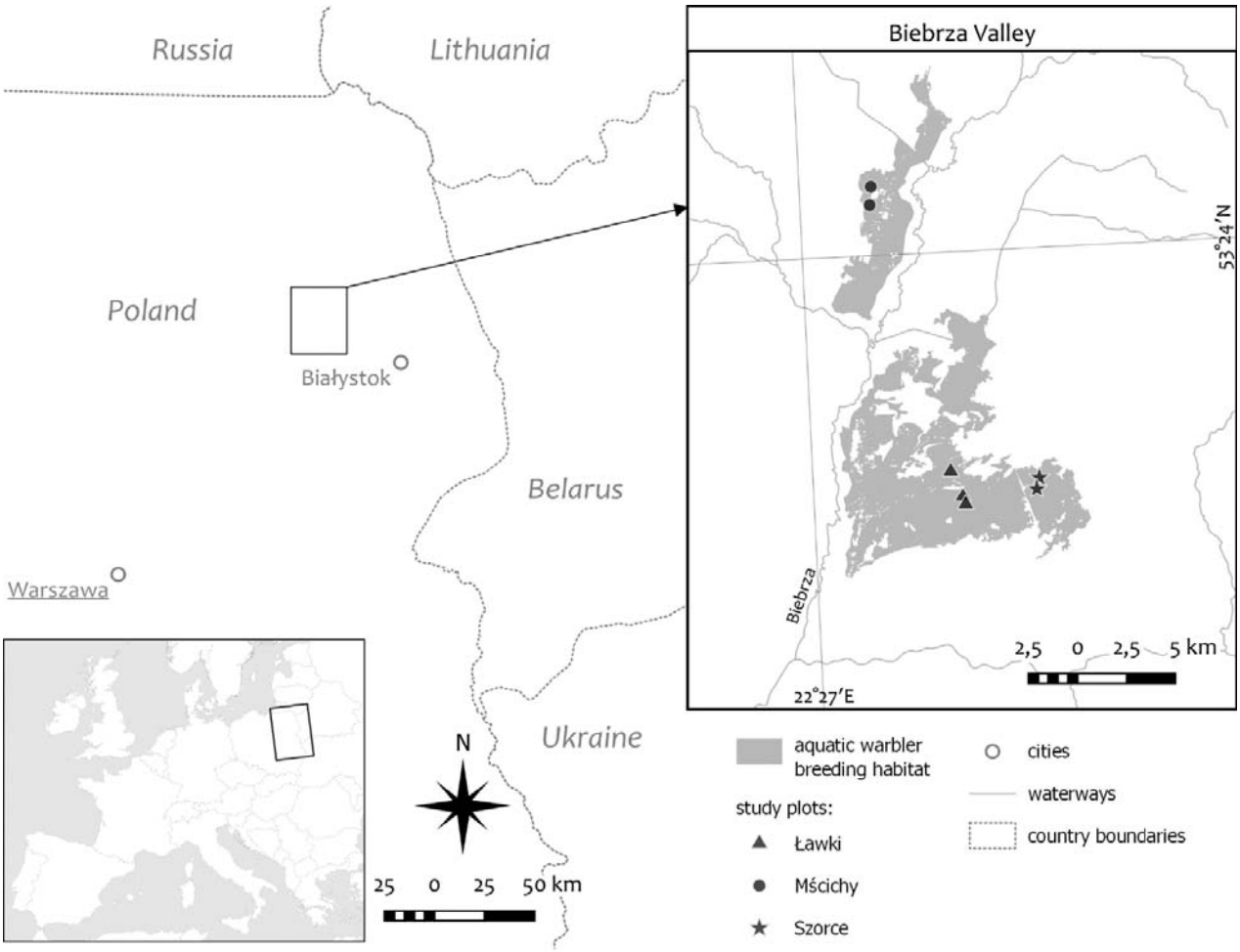


**Fig. 1** Map of the study area.

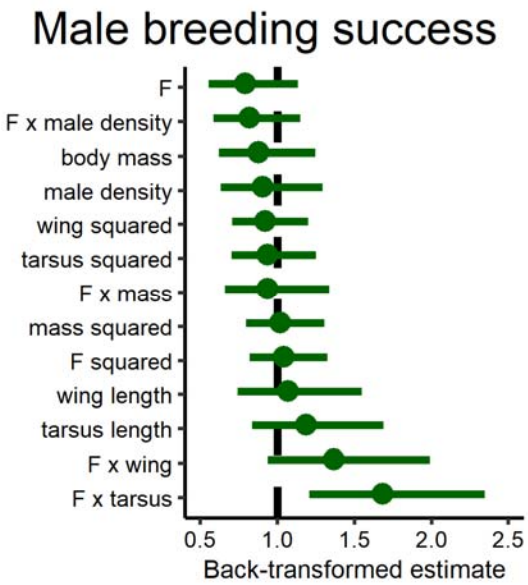


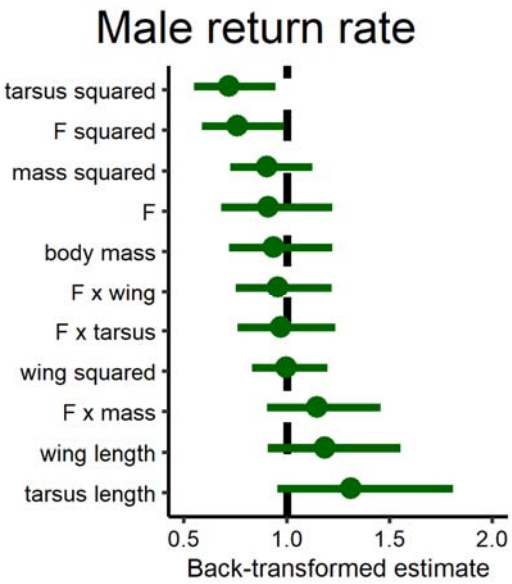


**Fig. 2** The estimates (denoted by circles) of effects of the male inbreeding coefficient *F*, phenotypic variables and their interaction with *F* on male fitness components: 4-year return rate to breeding grounds (left) and seasonal breeding success (right). The whiskers represent 95% confidence intervals and the vertical dashed line refers to no effect. See Table S3 for the summary of the estimates.

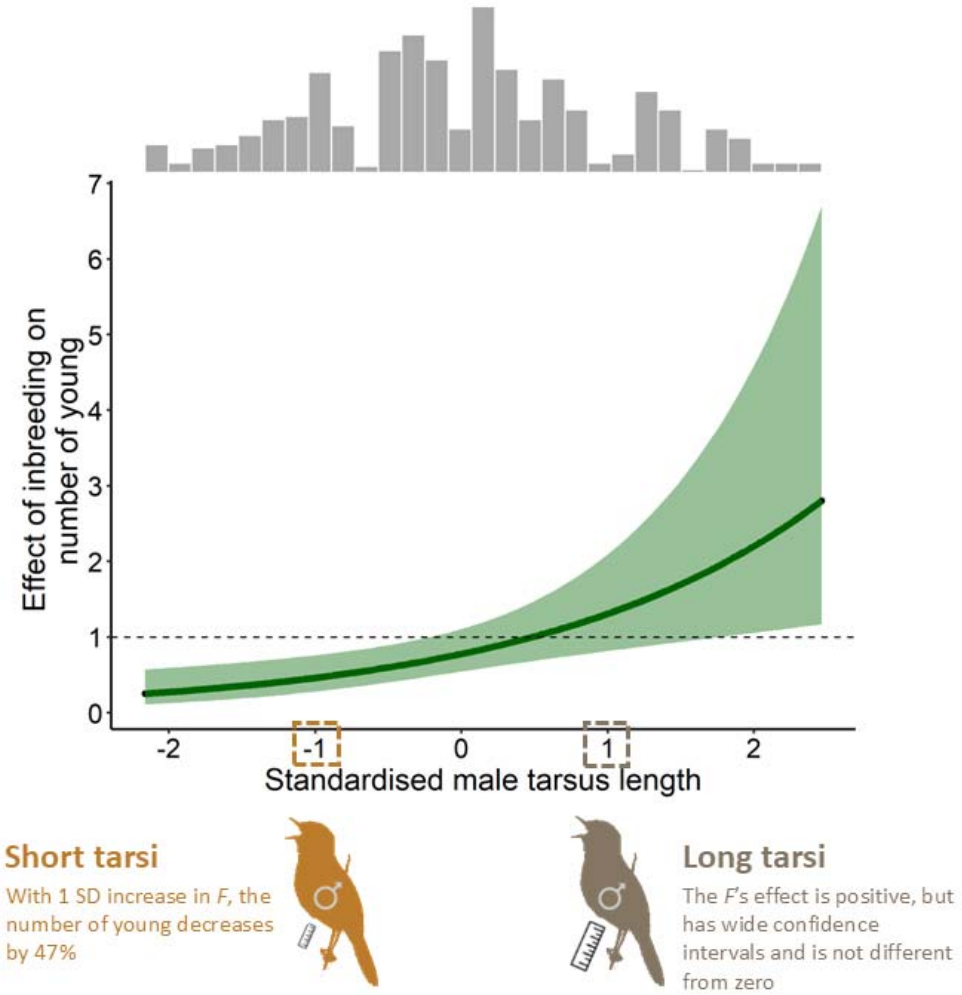


**Fig. 3** The effect of interaction between the male tarsus length and inbreeding coefficient *F* on the seasonal breeding success. The graph shows how the back-transformed statistical effect of *F* changes against standardised tarsus lengths, and the bands show the 95% confidence interval of the effect. The aquatic warbler pictograms at −1SD and +1SD present examples of how to interpret the graph. The horizontal dashed line corresponds to no effect. The histogram shows frequency of tarsus lengths.

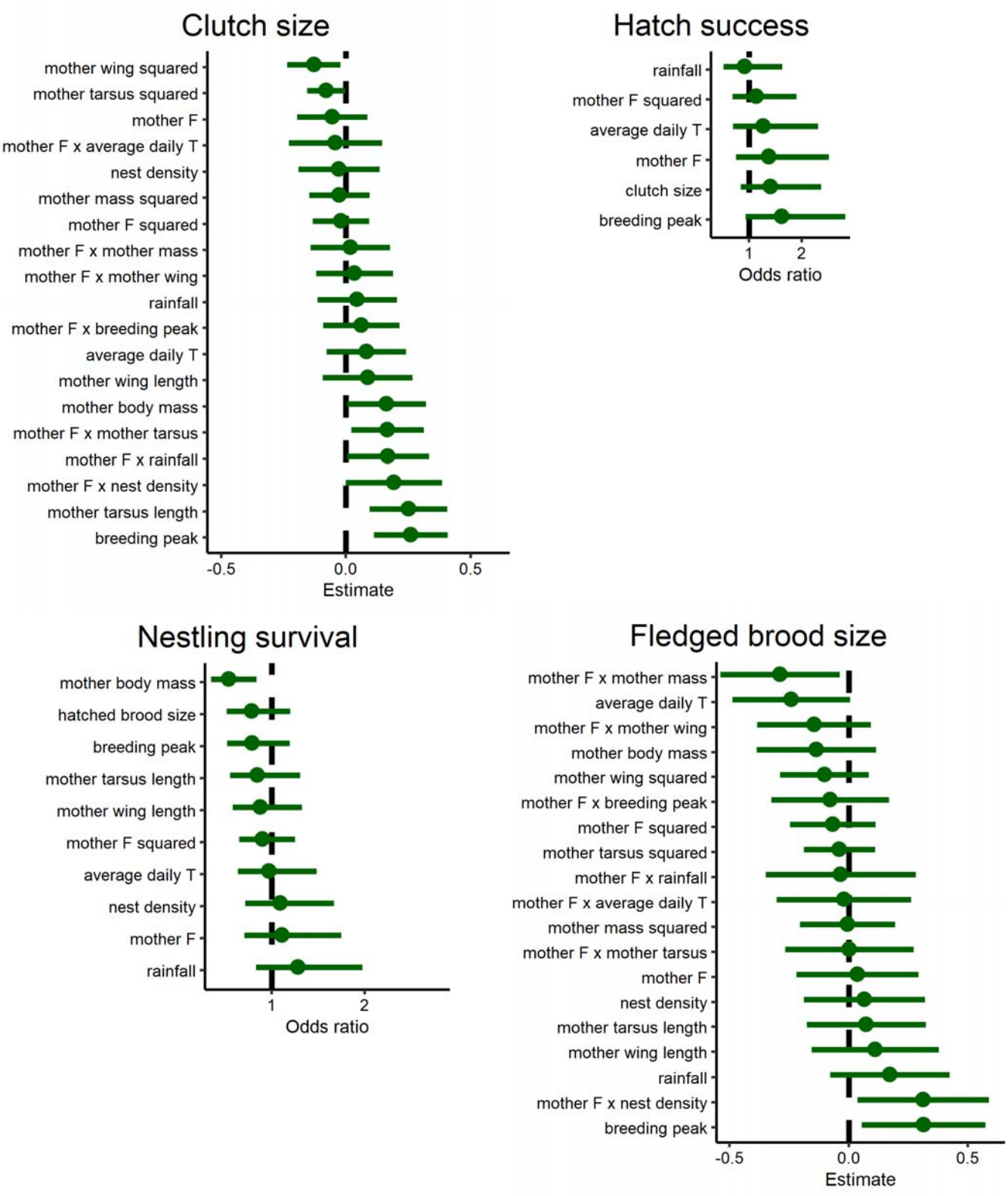


**Fig. 4** The estimates (denoted by circles) of effects of the mother inbreeding coefficient *F*, phenotypic variables and environmental variables and their interaction with *F* on female fitness components. The whiskers represent 95% confidence intervals and the vertical dashed line refers to no effect. See Table S5 for the summary of the estimates.

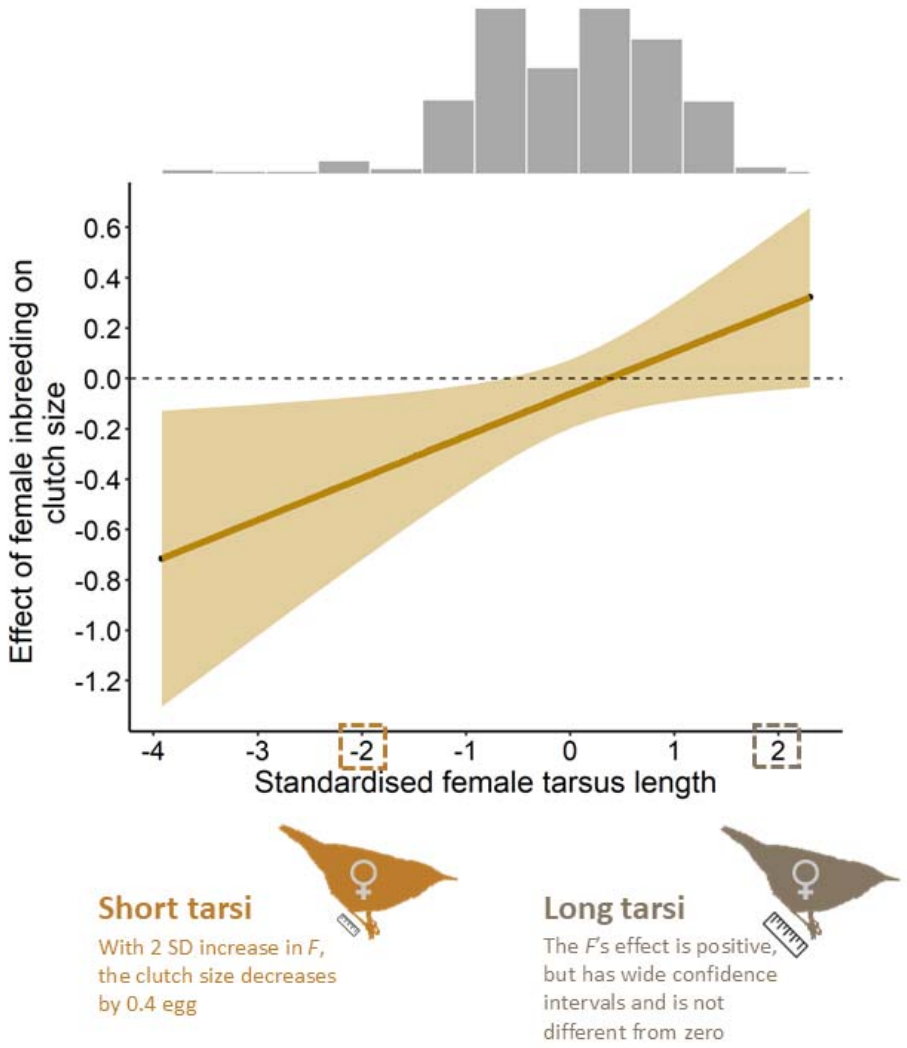


**Fig. 5**. The effect of interaction between the mother tarsus length and inbreeding coefficient *F* on the clutch size. The graph illustrates how the statistical effect of the mother *F* changes along the value of the tarsus. The aquatic warbler pictograms at –2 SD and +2 SD present examples of how to interpret the graph. The bands show the 95% confidence interval of the effect, the horizontal dashed line corresponds to no effect, and the histogram shows the frequency of tarsus lengths.

902

903 **Table 1.** Inbreeding load (*B*) and change in the fitness components due to inbreeding ($\delta$).

| Fitness component | Inbreeding determined in: | | Standardised *B* | Native scale *B* | Change in trait $-\delta$ |
|---|---|---|---|---|---|
| Male long-term survival | adult male | | 0.11[1] | 2.45[1] | −48.3%[1] |
| Male seasonal breeding success | adult male | | 0.21[1] | 4.87[1] | −69.3%[1] |
| Average small males | adult male | | 0.40[1] | 9.27[1] | −89.4%[1] |
| Average large males | adult male | | 0.01[1] | 0.21[1] | −5.0%[1] |
| Clutch size | adult female | | 0.06 | 1.26 | −5.0% |
| Average small females | adult female | | 0.12 | 2.83 | −11.5% |
| Average large females | adult female | | −0.01 | −0.28 | +1.1% |
| Hatch failure | adult female | | −0.01[2] | −0.17[2] | +3.5%[2] |
| Nestling mortality | adult female | | 0.01[2] | 0.15[2] | −2.9%[2] |
| Fledged brood size in successful nests | adult female | | −0.03 | −0.66 | +3.4% |

904 The *B* is expressed in lethal haploid equivalents and was calculated from weighted-averaged
905 predictions (Keller & Waller 2002, Box 3, Eqn II) of respective candidate model sets (Tables S2, S4 &
906 S6) on the link scale, which were then weighted-averaged between the study areas, years and
907 breeding peaks (if applicable). The native scale *B* was calculated by back-standardisation. The $\delta$ is
908 reported as the change in fitness of the most inbred relative to the least inbred individuals in the
909 dataset, and was calculated as above, with the final predictions back-transformed to the response
910 scale. For clarity, $-\delta$ is given, i.e. the minus in front of the $\delta$ means a decrease in the trait value,
911 while the plus indicates an increase.
912
913 [1] negative binomial distribution with log-link used
914 [2] poisson distribution with log-link used
915

916

917

918